Solid Freeform Fabrication 2018: Proceedings of the 29th Annual International Solid Freeform Fabrication Symposium – An Additive Manufacturing Conference
Reviewed Paper

PRECISION ENHANCEMENT OF 3D PRINTING VIA IN SITU METROLOGY

L. Li*, R. McGuan*, P. Kavehpour*, and R. N. Candler*†‡

*Department of Mechanical and Aerospace Engineering, University of California, Los Angeles, CA 90095
†Department of Electrical and Computer Engineering, University of California, Los Angeles, CA 90095
‡California Nano Systems Institute, Los Angeles, CA 90095
rcandler@g.ucla.edu

Abstract

The field of additive manufacturing, especially 3D printing, has gained growing attention in the research and commercial sectors in recent years. Notwithstanding that the capabilities of 3D printing have moved on to enhanced resolution, higher deposition rate, and a wide variety of materials, the crucial challenge of verifying that the component manufactured is within the dimensional tolerance as designed continues to exist. This work developed and demonstrated an approach for layer-by-layer mapping of 3D printed parts, which can be used for validation of printed models and *in situ* adjustment of print parameters. A high-speed optical scanning system was integrated with a Fused Deposition Modeling type 3D printer to scan during the print process on demands.

Keywords: Metrology, additive manufacturing, high-speed optical scanning, *in situ* validation, scan while printing, geometric dimensioning and tolerating.

Introduction

Additive manufacturing (AM) has been broadly utilized to fabricate parts in free-form shapes with internal cavities, which are normally not practicable or are highly priced using conventional machining procedures. One of the challenges that hinders the extensive use of AM in manufacturing is that 3D printed parts suffer from poor consistency of geometric dimensioning and tolerating (GD&T). In traditional manufacturing industries, products are put through the requirements of the geometry specification (ISO 10303 [1]), tolerances (ISO 1101 [2] and ASME Y14.5 [3]), and surface finish to ensure the functionality. In AM, however, the differences in the manufacturing process compared to traditional methods (e.g., build direction, layer thickness, etc.) and current limitations of AM processes make it difficult to achieve and maintain the specification and tolerance of complex freeform surfaces and internal functional features [4].

Many nondestructive (NDT) methods have been reported to evaluate the quality of additive manufactured parts, including using X-ray microcomputed tomography (microCT) [5-18], thermal [19-27], acoustic [28-30], image-based [31-35], and laser [36-40] sensors. MicroCT has been increasingly accepted in AM in recent years to measure porosity [6, 8-11], volume density [12], dimensional accuracy [13-15], and internal structures [7, 15-17]. The downsides to the more extensively implement of this technique are limited part size (especially for metal parts), minimum detectable pore size, and costs [5]. Although strategies for effective use of microCT have been well summarized in [18], this technique can only be used for post-build analysis. Thermal sensors (like pyrometers [19-23] or IR cameras [22-26]) have been used to capture thermographic images of printed object *in situ* to study the evolution and mechanisms of porosity and deformation [27]. Acoustic method, as known as acoustic emission (AE) [28] or spatially resolved acoustic spectroscopy (SRAS) [29] has been considered to be suitable for *in situ* quality monitoring for the diagnosis of surface and near-subsurface feature [30] due to its high sensitivity to the dynamic changes of mechanical systems. A sensitive acoustic emission sensor (like a fiber Bragg grating sensor) was used to qualify parts with different types and concentrations of pores with a sub-layer spatial resolution [28] *in situ* and in real time. However, thermal and acoustic techniques were only used to determine the existence and classify the type of the defect but barely describe its geometric information.

Image sensing systems are most broadly used for *in situ* real-time monitoring in AM. Three-dimensional shape of the printed part can be reconstructed by: 1) extracting and stacking features from images of different layers taken by a single high-speed high-resolution camera [31-33]; 2) using digital image correlation (DIC) technique to calculate the surface profile (height) of each layer from images taken by two cameras [34]. Delli et al. [35] reported a quality monitoring method for a Fused Deposition Modeling (FDM) or Fused Filament Fabrication (FFF) type 3D printer using a single camera and a supervised machine learning method called support vector machine (SVM). Images taken during printing were processed to classify the parts into 'good' or 'defective' category. However, images of each layer only provided limited information in 2D and it is computationally expensive and time consuming to reconstruct parts with complex shapes and precise features in 3D. Thus, a single-camera based image sensing system is not suitable to work with a closed-loop control system for real-time correction. Holzmond et al. [34] reported a "certify-as-you-build" quality assurance system which can capture the geometry of parts for each printed layer using 3D-DIC and detect print errors *in situ*. However, the major source of error also came from the 3D-DIC technique, including low correlation of images due to very high reflectivity of the surface and accuracy depending on system settings (such as lighting conditions, speckle/material grain pattern, focus, camera used, etc), which makes this approach not reliable for long-time monitoring of AM processes with various types of materials.

Recently, analysis of laser-scanned 3D point cloud data has been reported by several groups for the characterization of part geometric accuracy. Tootooni et al. [36] used a laser scanner (NextEngine) to scan a FDM fabricated part post build and developed a spectral graph approach working with six machine learning techniques (including sparse representation, k-nearest neighbors, NN, naïve Bayes, SVN, and decision tree) to classify overall dimensional variation (with classification accuracy F-score > 97%) by only sampling less than 5% of 2 million sample points. Although this method dramatically reduces measurement time and data processing burden, types of geometric deviation (e.g. direction and magnitude.) cannot be traced. Thus, Khanzadeh et al. [37] used an unsupervised machine learning approach called self-organizing map to fully quantify the link between geometric accuracy and AM process conditions from only 3% of the similar sets of data. However, this method only associates two process parameters (extruder temperature and infill percentage) with direction and magnitude of deviation. And the sampling reduction is based on the analysis of a full set of scanned data which means a test part must be built and scanned for a new design. Besides, these two groups only scanned the part post build which means only the geometry of the outside surface was examined. Lu et al. [38] and Sitthi-Amorn et al. [39] used laser scanners to scan each finished layer and used the height profile as feedback for a closed-loop control system to achieve *in situ* self-correction for ink-jet 3D printers. Guo et al. [40-41] developed more advanced models to predict the layer height profile after deposition and mentioned that it took 3 to 5 seconds to calculate one printing layer. Notwithstanding, their control-oriented models only work for droplet-based printers.

More recently, we have integrated a high-resolution optical scanning system with a FDM type 3D printer to scan during the print process on demands. An approach for layer-by-layer mapping of 3D printed parts is developed and demonstrated, which can be used for understanding the influence of a full set of factors (such as printing parameters, material properties, and environmental factors) to the part quality using machine learning, validation of printed objects *in situ,* and self-adjustments of printing process by developing and implementing a real-time closed-loop control system. The main advantages of this work are that: 1) an advanced laser confocal displacement sensor was used in the system to achieve sub-micron resolution of the scanned profile; 2) the optical sensor was fully integrated with the 3d printer, and the scanning was executed during printing without extra post-processing measurement; 3) the scanning path and sampling rate can be customized to fit specific applications and tune the tradeoff between scan time and resolution.

Method

1. System Setup

The system setup is shown in Figure 1 (a). A FDM type 3D printer (System 30M, Hyrel International Inc., GA, USA) with 50 μm position accuracy in the X/Y-axis and 10 μm in the Z-axis was used with a MK1-250 hot flow print head with 0.5 mm nozzle to print ABS filament feedstock with 1.75 mm diameter. The key component of the system is a surface scanning laser confocal displacement meter (LT-9030M, Keyence Corporation, IL, USA), which has a measurement range of ±1.0 mm from the reference position (30 mm below the bottom of sensor) with resolution of 0.1 μm. The laser sensor is held by a custom-designed sensor holder (as shown in Figure 1 (b)) which is inserted in one of the head slots of the 3D printer. Thus, the laser beam is perpendicular to the building stage and is able to move during the printing process without using extra actuators. The resolution of the measurement system is limited by not only the resolution of the laser sensor but also the position accuracy of the printer. The Z and X/Y coordinates of the scanned surface profile were collected from the laser sensor and the 3D printer correspondingly using a data acquisition board (USB 6008, National Instruments, TX, USA) under the control of a LabVIEW program.

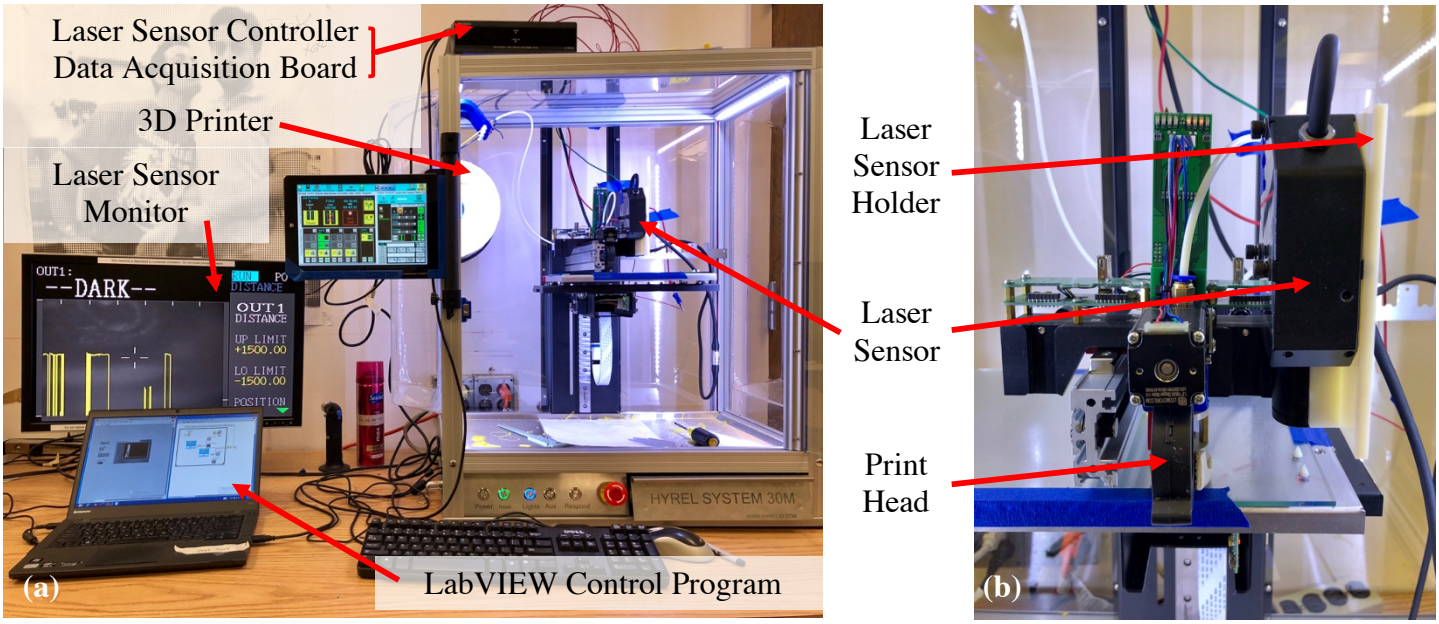

Figure 1 (a) A picture of the essential components of the system. (b) A zoomed in picture shows the laser sensor moves in parallel with the print head during the printing/scanning process.

2. Scanning While Printing

A schematic of the system is shown in Figure 2. The scanning process runs between printing of layers and is achieved by modifying the tool path (also known as the G-code, the most widespread Computer Numerical Control (CNC) programming language) of the print head. In other words, code is written to make the printer think that the confocal sensor is a print head, such that all the built-in functions for print head control can be leveraged for controlling the scanner. The printed filament width was 0.55 mm and each layer was 0.2 mm thick. The moving velocities of the print head and the laser sensor were set at 1800 and 300 mm/min, respectively. The scan path used in this work is a snaking pattern which passes by every point of intersection of a rectangular grid covering the largest area in plane with both X and Y separation of 0.1 mm or 0.5 mm. A sacrificial pattern was printed aside the formal part to consume and remove the redundant material that was observed to drip while the print head waited during the scanning process. Depending on the specific printer being used, this sacrificial pattern may not always be required.

Some approaches can be performed to reduce the current ~6:1 scan:print time ratio.

- Increase the moving speed of the laser sensor to as high as 1800 mm/min, which can decrease the scan time to 1/6. However, the moving speed of the laser sensor is limited by the sampling rate of the DAQ device and scan path separation to avoid over/undersampling issues.
- The laser sensor used in this work is only capable of measuring 1D displacement (Z coordinate) and the moving speed in plane is slow compared to intrinsic scanning speed of more advanced laser scanners. For example, to scan a 7 mm x 7 mm area with scan separation of 0.1 mm in both X and Y axis, the total number of points, which the printer needs to move the laser sensor to, is 4900 using an 1D laser scanner (Keyence LT-9030M). And the total numbers of points are 70 using a 2D laser scanner (Keyence LJ-V7020 with X-axis measurement range of 7 mm) and 1 using a 3D laser scanner (Keyence WI-010 with XY measurement range of 10 mm x 10 mm) without sacrificing resolution in Z axis. Thus, the scan time can be decreased to 1/4900 by using a more advanced laser scanner.
- Custom design scan path to focus more on interesting features (like boundaries) and leverage the resolution and time of the scanning process if overall time needs to be optimized. Symmetry of the CAD model and G-code can be utilized to further reduce the scan burden.

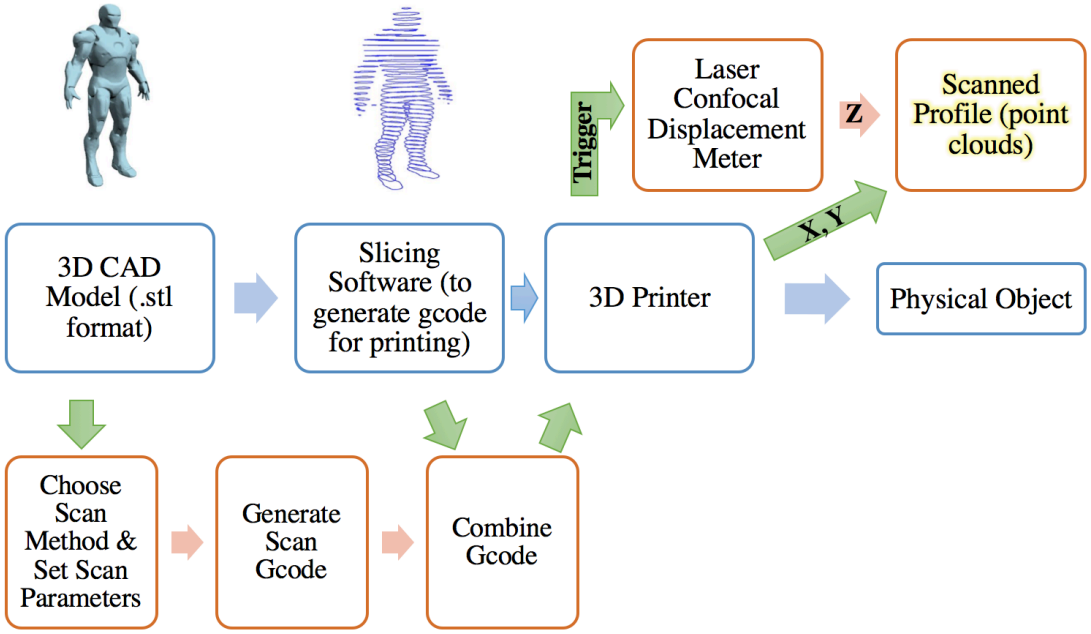

Figure 2 A schematic of the system. Blue blocks show the standard workflow of AM. Orange blocks show the extra work to achieve scanning while printing.

Initial Results

Three sets of scanning while printing tests were conducted on solid parts with simple geometries, their correlated hollow parts, and an object with both complicated geometry and hollow structures.

1. Simple Solid Parts

A solid cuboid, a cylinder, a bottom half sphere, and a thin wall with characteristic lengths of 5 mm and thicknesses of 3 mm were scanned after every three layers. The scanned point clouds in comparison with CAD models are shown in Figure 3. The light blue points at the bottom represent the scanned surface of the adhesion layer between parts and the build stage.

Based on the comparisons, several aspects of the part geometries were not maintained during the printing process. The right-angle corners of the cuboid and the thin wall were rounded due to the continuous extrusion of the filaments. The side walls of all four parts were wavy due to the slightly different volumes of extrusion of the filaments, various shrinkage of each printed layer and positional inaccuracy of the 3D printer. The issues worsened for the half bottom sphere part with the negative side wall and the thin wall part with large aspect ratio. Some undesired features beside the parts (as shown in the pictures) were from leakage of filament from the print head during scanning because the sacrificial patterns were not put far enough from the scanned objects.

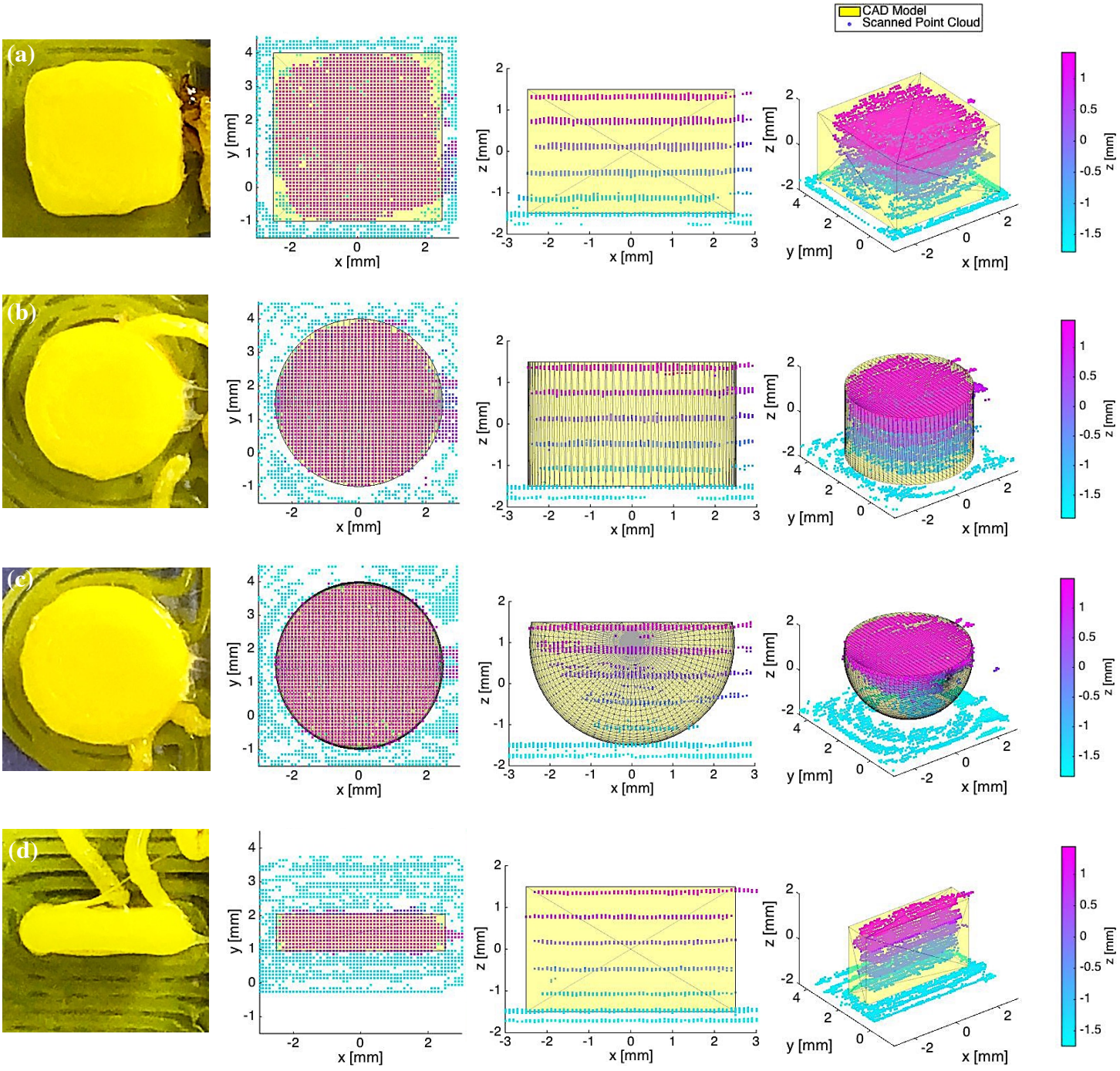

Figure 3 Pictures and scanned point clouds (in the top, side, and 3D views) in comparison with the corresponding CAD models of the solid (a) cuboid, (b) cylinder, (c) bottom half sphere, and (d) thin wall.

2. Simple Hollow Parts

Parts with same outside geometries as those in the previous section were hollowed in the center and the thickness of the shells left was 1.1 mm. The scanned point clouds in comparison with CAD models are shown in Figure 4. The printed part shrank less where its center was hollow which led to a larger top compared to its bottom. Also, the geometries of the internal structures also showed deviation from the designs.

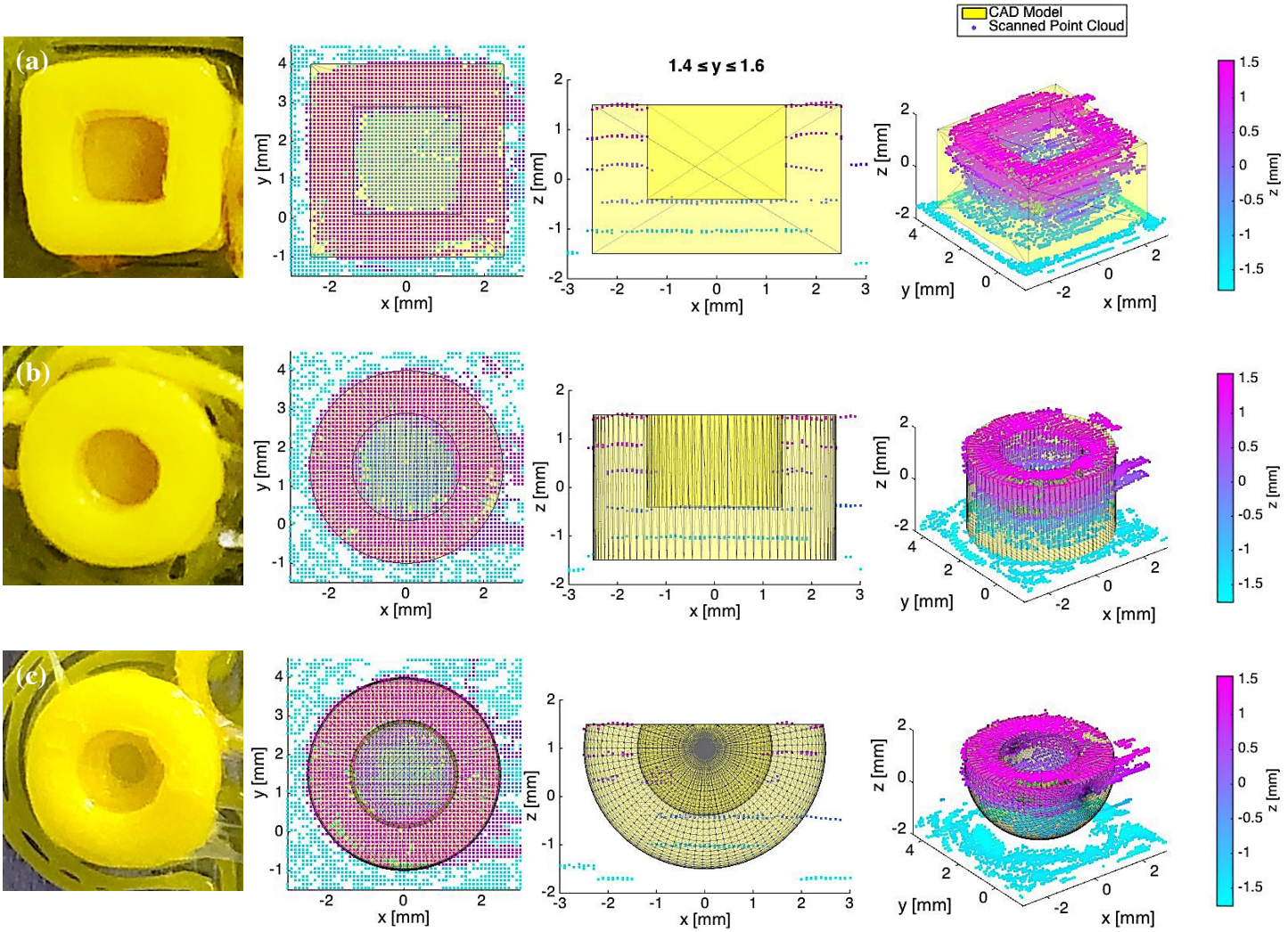

Figure 4 Pictures and scanned point clouds (in the top, side with 1.4 ≤ y ≤ 1.6, and 3D views) in comparison with the corresponding CAD models of the hollow (a) cuboid, (b) cylinder, and (c) bottom half sphere.

3. Complicated Hollow Part

A partial Kaplan turbine with a logo that rotated through the structure thickness was printed and scanned every 5 layers in order to investigate a structure with complex features. The scan path separations in both X and Y axis were 0.5 mm. The scanned point clouds in comparison with CAD models are shown in Figure 5.

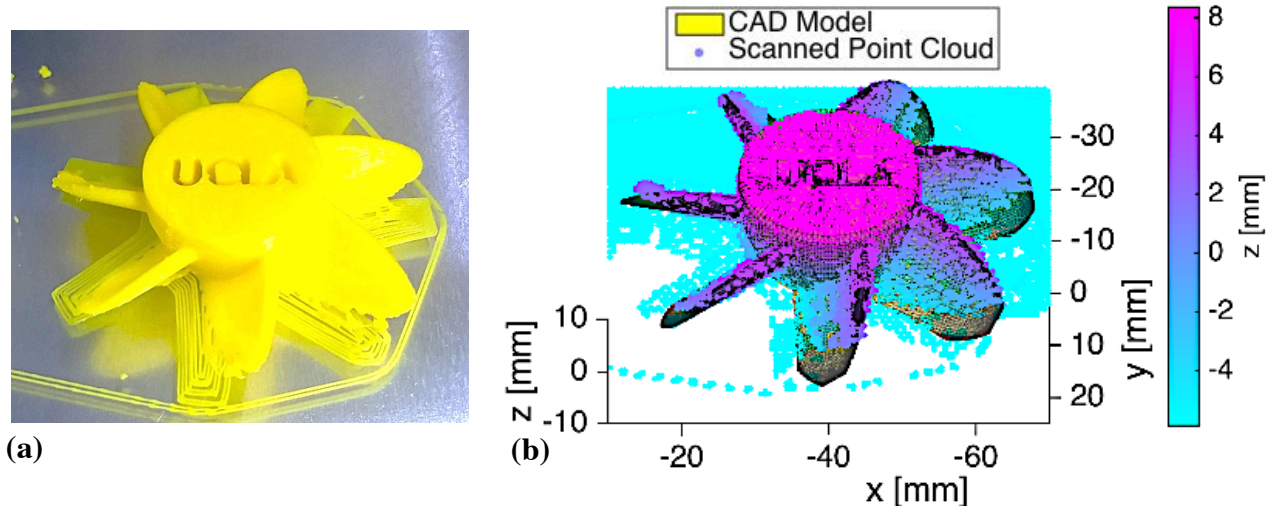

Figure 5 Pictures and scanned point clouds in comparison with the corresponding CAD models of the complicated hollow part.

To get a better view of the inside structures, the scanned point cloud was sliced into four horizontal planes at different heights (from top to bottom) as shown in Figure 6.

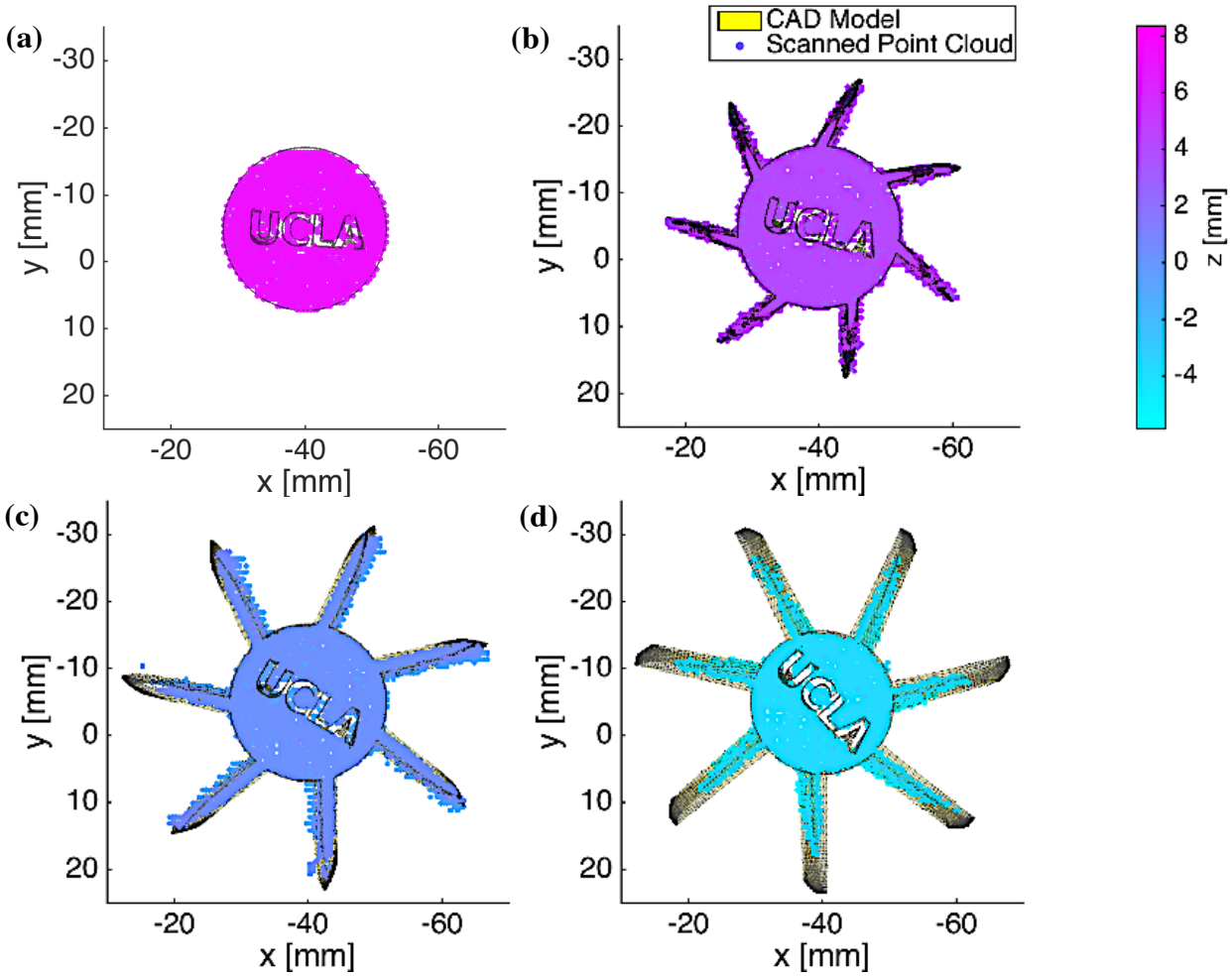

Figure 6 Slices in the X-Y plane of the scanned point clouds of the complicated hollow part at (a) $6 \le z \le 8$, (b) $3 \le z \le 5$, (c) $-1 \le z \le 1$, and (d) $-5 \le z \le -3$.

Conclusion

A high-speed optical scanning system was integrated with an FDM type 3D printer to scan during the print process on demands. Four simple solid parts, three simple hollow parts, and one complicated hollow part have been successfully scanned during the printing process and mapped to the corresponding model based on a layer-by-layer basis. This system can be applied to understand the influence of a full set of factors (such as printing parameters, material properties, and environmental factors) to the part quality using machine learning, validate printed objects *in situ,* and self-adjust the printing process by developing and implementing a real-time closed-loop control system. In the future, we plan to 1) use advanced point cloud processing tools (such as Point Cloud Library, The 3D Toolkit, and Point Data Abstraction Library) to fully recognize the features of different kinds of defects (like gaps, curling, blobs and zits, etc.), 2) implement machine learning models to identify the relationships of input factors and defect formation mechanisms, and 3) develop a real-time closed-loop control system to self-correct the defects *in situ* and realize a 'born-as-qualified' printing process.

Acknowledgments

This work was supported by the Navy as part of the NEEC program, Award No. N00174-17-1-0004, under the NEEC mentorship of Doug Sugg, Aaron Wiest, and Subrata Sanyal.

References

[1] ISO, S. A. H., 2006, STEP Application Handbook, SCRA, North Charleston, SC.
[2] ISO 1101:2012, 2012, Geometrical Product Specifications (GPS)—Geometrical Tolerancing—Tolerances of Form, Orientation, Location and Run-Out, ISO, Geneva, Switzerland.
[3] ASME Y14.5-2009, 2009, Dimensioning and Tolerancing, ASME, New York.
[4] Lipman, R., Moylan, S., Witherell, P., 2015. Investigating the Role of Geometric Dimensioning and Tolerancing in Additive Manufacturing.
[5] Thompson A, Maskery I, Leach RK. X-ray computed tomography for additive manufacturing: A review. Meas Sci Technol 2016;27:072001.
[6] Khairallah SA, Anderson AT, Rubenchik A, et al. Laser powder-bed fusion additive manufacturing: Physics of complex melt flow and formation mechanisms of pores, spatter, and denudation zones. Acta Mater 2016;108: 36–45.
[7] Grasso M, Demir AG, Previtali B, et al. In situ monitoring of selective laser melting of zinc powder via infrared imaging of the process plume. Robot Comput Integr Manuf 2018;49:229–239.
[8] Yadroitsau I. Selective Laser Melting: Direct Manufacturing of 3D-Objects by Selective Laser Melting of Metal Powders. Saarbrucken, Germany: LAP LAMBERT Academic Publishing, 2009.
[9] Cacace S, Demir AG, Semeraro Q. Densification mechanism for different types of stainless steel powders in selective laser melting. Procedia CIRP 2017;62:475–480.
[10] Chen H, Wei Q, Wen S, et al. Flow behavior of powder particles in layering process of selective laser melting: Numerical modeling and experimental verification based on discrete element method. Int J Mach Tools Manuf 2017; 123:146–159.
[11] Tan JH, Wong WLE, Dalgarno KW. An overview of powder granulometry on feedstock and part performance in the selective laser melting process. Addit Manuf 2017;18: 228–255.
25.
[12] du Plessis A, Meincken M, Seifert T. Quantitative determination of density and mass of polymeric materials using microfocus computed tomography. J Nondestruct Eval 2013;32:413–417.
[13] Villarraga-Go´mez H, Lee C, Smith ST. Dimensional metrology with X-ray CT: A comparison with CMM measurements on internal features and compliant structures. Precis Eng 2018;51:291–307.
[14] Ferrucci M, Leach RK, Giusca C, et al. Towards geo- metrical calibration of x-ray computed tomography systems—A review. Meas Sci Technol 2015;26:92003.

[15] Snyder JC, Stimpson CK, Thole KA, et al. Build direction effects on microchannel tolerance and surface roughness. J Mech Des 2015;137:111411.
[16] Karme A, Kallonen A, Matilainen VP, et al. Possibilities of CT scanning as analysis method in laser additive manufacturing. Phys Procedia 2015;78:347–356.
[17] Thompson A, Senin N, Maskery I, et al. Internal surface measurement of metal powder bed fusion parts. Addit Manuf 2018;20:126–133.
[18] du Plessis, A., Yadroitsev, I., Yadroitsava, I., Le Roux, S.G., 2018. X-Ray Microcomputed Tomography in Additive Manufacturing: A Review of the Current Technology and Applications. 3D Print. Addit. Manuf. 00, 3dp.2018.0060.
[19] M. Doubenskaia, A. Domashenkov, I. Smurov, Study of the laser melting of pre-deposited intermetallic TiAl powder by comprehensive optical diagnostics, Surf. Coat. Technol. 321 (2017) 118–127.
[20] W. Devesse et al., High resolution temperature estimation during laser cladding of stainless steel, in: Laser Assisted Net Shape Engineering 9 International Conference on Photonic Technologies Proceedings of the Lane 2016, 2016, 83, pp. 1253–1260.
[21] I. Smurov et al., Optical monitoring in laser cladding of Ti6Al4V, J. Therm. Spray Technol. 21 (6) (2012) 1357–1362.
[22] I. Smurov, M. Doubenskaia, A. Zaitsev, Comprehensive analysis of laser cladding by means of optical diagnostics and numerical simulation, Surf. Coat. Technol. 220 (2013) 112–121.
[23] M. Doubenskaia et al., Complex analysis of elaboration of steel–TiC composites by direct metal deposition, J. Laser Appl. 25 (4) (2013) 042009.
[24] H. Krauss, T. Zeugner, M.F. Zaeh, Layerwise monitoring of the selective laser melting process by thermography, Phys. Proc. 56 (2014) 64–71.
[25] S. Moylan et al., Infrared thermography for laser-based powder bed fusion additive manufacturing processes, in: 40th Annual Review of Progress in Quantitative Nondestructive Evaluation: Incorporating the 10th International Conference on Barkhausen Noise and Micromagnetic Testing, vols. 33a & 33b, 2014, 1581, pp. 1191–1196.
[26] U. Hassler et al., In-situ monitoring and defect detection for laser metal deposition by using infrared thermography, Phys. Proc. 83 (2016) 1244–1252.
[27] Yan, Z., Liu, W., Tang, Z., Liu, X., Zhang, N., Li, M., Zhang, H., 2018. Review on thermal analysis in laser-based additive manufacturing. Opt. Laser Technol. 106, 427–441.
[28] Shevchik, S.A., Kenel, C., Leinenbach, C., Wasmer, K., 2018. Acoustic emission for in situ quality monitoring in additive manufacturing using spectral convolutional neural networks. Addit. Manuf. 21, 598–604.
[29] Hirsch, M., Patel, R., Li, W., Guan, G., Leach, R.K., Sharples, S.D., Clare, A.T., 2017. Assessing the capability of in-situ nondestructive analysis during layer based additive manufacture. Addit. Manuf. 13, 135–142.
[30] R.J. Smith, M. Hirsch, R. Patel, W. Li, A.T. Clare, S.D. Sharples, spatially resolved acoustic spectroscopy for selective laser melting, J. Mater. Process. Technol. (2016).
[31] J. zur Jacobsm¨uhlen, S. Kleszczynski, D. Schneider, and G. Witt, "High resolution imaging for inspection of laser beam melting systems," in Instrumentation and Measurement Technology Conference (I2MTC), 2013 IEEE International. IEEE, 2013, pp. 707–712.
[32] B. Foster, E. Reutzel, A. Nassar, B. Hall, S. Brown, and C. Dickman, "Optical, layerwise monitoring of powder bed fusion," in Solid Free. Fabr. Symp. Proc, 2015, pp. 295–307.
[33] M. Grasso, V. Laguzza, Q. Semeraro, and B. M. Colosimo, "In-process monitoring of selective laser melting: Spatial detection of defects via image data analysis," Journal of Manufacturing Science and Engineering, vol. 139, no. 5, p. 051001, 2017.
[34] Hammond, O., Li, X., 2017. In situ real time defect detection of 3D printed parts. Addit. Manuf. 17, 135–142.
[35] Delli, U., Chang, S., 2018. Automated Process Monitoring in 3D Printing Using Supervised Machine Learning. Procedia Manuf. 26, 865–870.

[36] Samie Tootooni, M., Dsouza, A., Donovan, R., Rao, P.K., Kong, Z. (James), Borgesen, P., 2017. Classifying the Dimensional Variation in Additive Manufactured Parts From Laser-Scanned Three-Dimensional Point Cloud Data Using Machine Learning Approaches. J. Manuf. Sci. Eng. 139, 091005.
[37] Khanzadeh, M., Rao, P., Jafari-Marandi, R., Smith, B.K., Tschopp, M.A., Bian, L., 2017. Quantifying Geometric Accuracy With Unsupervised Machine Learning: Using Self-Organizing Map on Fused Filament Fabrication Additive Manufacturing Parts. J. Manuf. Sci. Eng. 140, 031011.
[38] Lu, L., Zheng, J., Mishra, S., 2015. A layer-to-layer model and feedback control of ink-jet 3-D printing. IEEE/ASME Trans. Mechatronics 20, 1056–1068.
[39] Sitthi-amorn, P., Lan, J., Wang, W., 2015. MultiFab: A Machine Vision Assisted Platform for Multi-material 3D Printing. ACM Trans. Graph. 11.
[40] Guo, Y., Mishra, S., 2016. A predictive control algorithm for layer-to-layer ink-jet 3D printing. Proc. Am. Control Conf. 2016–July, 833–838.
[41] Guo, Y., Peters, J., Oomen, T., Mishra, S., 2018. Control-oriented models for ink-jet 3D printing. Mechatronics 0–1.